Gating and Flickery Block Differentially Affected by Rubidium in Homomeric KCNQ1 and Heteromeric KCNQ1/KCNE1 Potassium Channels

Michael Pusch, Lara Bertorello, and Franco Conti
Istituto di Cibernetica e Biofisica, Consiglio Nazionale della Ricerche, Via de Marini 6, I-16149 Genova, Italy

ABSTRACT The voltage-gated potassium channel KCNQ1 associates with the small KCNE1 subunit to form the cardiac IKs delayed rectifier potassium current and mutations in both genes can lead to the long QT syndrome. KCNQ1 can form functional homotetrameric channels, however with drastically different biophysical properties compared to heteromeric KCNQ1/KCNE1 channels. We analyzed gating and conductance of these channels expressed in *Xenopus* oocytes using the two-electrode voltage-clamp and the patch-clamp technique and high extracellular potassium (K) and rubidium (Rb) solutions. Inward tail currents of homomeric KCNQ1 channels are increased about threefold upon substitution of 100 mM potassium with 100 mM rubidium despite a smaller rubidium permeability, suggesting an effect of rubidium on gating. However, the kinetics of tail currents and the steady-state activation curve are only slightly changed in rubidium. Single-channel amplitude at negative voltages was estimated by nonstationary noise analysis, and it was found that rubidium has only a small effect on homomeric channels (1.2-fold increase) when measured at a 5-kHz bandwidth. The apparent single-channel conductance was decreased after filtering the data at lower cutoff frequencies indicative of a relatively fast "flickery/block" process. The relative conductance in rubidium compared to potassium increased at lower cutoff frequencies (about twofold at 10 Hz), suggesting that the main effect of rubidium is to decrease the probability of channel blockage leading to an increase of inward currents without large changes in gating properties. Macroscopic inward tail currents of heteromeric KCNQ1/KCNE1 channels in rubidium are reduced by about twofold and show a pronounced sigmoidal time course that develops with a delay similar to the inactivation process of homomeric KCNQ1, and is indicative of the presence of several open states. The single channel amplitude of heteromers is about twofold smaller in rubidium than in potassium at a bandwidth of 5 kHz. Filtering at lower cutoff frequencies reduces the apparent single-channel conductance, the ratio of the conductance in rubidium versus potassium is, however, independent of the cutoff frequency. Our results suggest the presence of a relatively rapid process (flicker) that can occur almost independently of the gating state. Occupancy by rubidium at negative voltages favors the flicker-open state and slows the flickering rate in homomeric channels, whereas rubidium does not affect the flickering in heteromeric channels. The effects of KCNE1 on the conduction properties are consistent with an interaction of KCNE1 in the outer vestibule of the channel.

INTRODUCTION

The cardiac action potential is mediated by a multitude of ion channels, and mutations in several cardiac ion channel genes can lead to the so-called long QT syndrome (LQTS) that is associated with cardiac arrhythmia (see Ackerman, 1998 for review). It is now well established that the slow cardiac outward-rectifier channel, IKs, is formed by a heteromultimeric association of KCNQ1, a potassium channel protein with the classical *Shaker*-like architecture composed of six transmembrane segments and a pore-forming P-loop invagination (Wang et al., 1996a; Yang et al., 1997), and the small one-transmembrane-segment protein KCNE1 (also called minK) (Takumi et al., 1988; Barhanin et al., 1996; Sanguinetti et al., 1996). Mutations in both subunits can cause LQT (Wang et al., 1996a; Splawski et al., 1997; Schulze-Bahr et al., 1997). Although KCNQ1 can form functional homomeric potassium channels in heterologous expression systems (Barhanin et al., 1996; Sanguinetti et al., 1996) heteromeric KCNQ1/KCNE1 channels have drastically different biophysical properties, and the fact that mutations in KCNE1 can cause LQT demonstrates that this subunit is essential for a proper function of IKs in the heart. In addition to changing the biophysical properties of the resulting potassium channel, another function of KCNE1/KCNQ1 coassembly could be to increase the number of functional channels in the plasma membrane, either by increasing the rate of synthesis or by decreasing the turnover rate. The following biophysical properties are altered when KCNQ1 is coexpressed with KCNE1: The activation time course is drastically slowed (Barhanin et al., 1996; Sanguinetti et al., 1996), an inactivation process present in homomeric channels is apparently eliminated (Pusch et al., 1998; Tristani-Firouzi and Sanguinetti, 1998), the single channel conductance is increased about threefold (Pusch, 1998; Yang and Sigworth, 1998; Sesti and Goldstein, 1998). It is not clear what mechanism underlies these drastic changes. Because of the increase of the single channel conductance and because mutations in KCNE1 can alter the ion selectivity (e.g., Goldstein and Miller, 1991; Wang et al., 1996b; Tai and Goldstein, 1998), several groups have

Received for publication 12 July 1999 and in final form 6 October 1999.
Address reprint requests to Michael Pusch, Istituto di Cibernetica e Biofisica, CNR, Via de Marini 6, I-16149 Genova, Italy. Tel.: +39-010-6475-561; Fax: +39-010-6475-500; E-mail: pusch@barolo.icb.ge.cnr.it.

0006-3495/00/01/211/16 $2.00

proposed that KCNE1 interacts with KCNQ1 directly in a pore-participating structure. Also, the accessibility to cadmium evidenced by a reduction of macroscopic current of cysteine-mutated KCNE1 was interpreted as a participation of KCNE1 to the pore (Tai and Goldstein, 1998). However, none of the above observations rules out the possibility that the effects of KCNE1 on open-channel properties are indirectly due to changes of the channel-complex probability for two or more open states with different selectivities and/or conductances.

To understand in more detail the similarities and differences in the gating and conductance of homomeric KCNQ1 and heteromeric KCNQ1/KCNE1 channels, we extended our previous results (Pusch et al., 1998) to measurements in high extracellular rubidium. It is well known that rubidium affects the gating of several potassium channels, slowing often the deactivation kinetics (e.g., Swenson and Armstrong, 1981; Cahalan et al., 1985; Matteson and Swenson, 1986; Sala and Matteson 1991; Shapiro and DeCoursey, 1991a,b). Rubidium is, therefore, a useful tool to investigate gating and conductance properties of potassium channels. We made the surprising finding that inward tail currents of homomeric KCNQ1 are drastically increased in high rubidium with only little changes of the single-channel conductance and kinetic parameters. In contrast, high rubidium decreases the inward tail currents and the single-channel conductance of heteromeric KCNQ1/KCNE1 channels by about the same factor while making the time course of the tail currents strongly sigmoidal and more reminiscent of the presence of an inactivation process similar to that found for homomeric channels.

To explain the hook in the tail currents of homomeric KCNQ1 channels, we have previously proposed a gating model that includes (at least) two open states and an intrinsically voltage-independent inactivation process coupled to channel opening (Pusch et al., 1998). The model was able to account for the delayed and incomplete inactivation of homomeric KCNQ1 that is responsible for the transient increase of the potassium conductance (hook) on repolarization after an activating prepulse. Our present results suggest the presence of an additional gating mechanism (flicker) that is affected by rubidium and by the association of KCNQ1 with KCNE1.

METHODS AND MATERIALS

cRNA synthesis and oocyte injection

Capped RNA was transcribed from human KCNQ1 and human KCNE1 as described (Pusch et al., 1998). About 10 ng KCNQ1 cRNA (for homomeric channels) or 5 ng KCNQ1 cRNA + 0.5 ng KCNE1 cRNA (for heteromeric channels) were injected per oocyte. Oocytes were injected and treated as described (Pusch et al., 1998). Injection of only KCNE1 into oocytes gives rise to potassium currents with similar properties as KCNQ1/KCNE1 channels (Takumi et al., 1988; Barhanin et al., 1996), and it is believed that the channels underlying this current are formed by the heteromeric association with an endogenous KCNQ1 subunit (Barhanin et al., 1996). The influence of this endogenous current was controlled by the following precautions. We routinely injected the same amount of KCNE1 RNA without KCNQ1 and compared the magnitude of the expressed currents after at least two days of expression. The magnitude of the current in coinjected oocytes was always much larger than in those injected only with KCNE1 (usually at least 10-fold larger) such that the contribution of the endogenous current could be largely neglected. In addition, we found that the currents measured after injection of only KCNE1 started to diminish after two days of expression, whereas the currents of co-injected oocytes continued to increase up to seven days after injection.

Recording solutions

The following solutions were used as bath solutions in whole-oocyte voltage-clamp recordings and as (extracellular) pipette solutions in cell-attached patch-clamp recordings (amounts are in mmol/l; Hepes = Na-*n*-[2-hydroxyethyl]piperazine-*n*′-[2-ethanesulfonic acid]; pH 7.3 for all solutions, titrated with NaOH):

100 K: 100 KCl, 0.5 $CaCl_2$, 3 $MgCl_2$, 5 Hepes;

100 Rb: 100 RbCl, 0.5 $CaCl_2$, 3 $MgCl_2$, 5 Hepes.

For cell-attached patch recordings, the oocyte was bathed in a high potassium low calcium solution such that the membrane potential could be assumed to be close to 0 mV as described (Pusch, 1998).

Electrophysiology and data analysis

Standard two-electrode voltage-clamp measurements were performed 2–5 days after injection at room temperature (22–24°C) using a homemade high-voltage amplifier, two 3-M KCl agar-bridges as extracellular voltage- and current-electrodes, and two 3-M KCl-filled intracellular pipettes with 0.5- to 1-MΩ resistance. Stimulation and data acquisition was performed with an Instrutech AD/DA interface and the Pulse-software (HEKA, Lambrecht/Pfalz, Germany) controlled by a Pentium-based computer. Cell-attached patches were used for measurements of nonstationary current fluctuations recorded at 18–19°C with an EPC7 patch-clamp amplifier (List, Darmstadt, Germany) as described (Pusch, 1998).

Voltage-clamp protocols are described in the figure legends. The holding potential in all recordings was −80 mV (except for the noise measurements of heteromeric channels). Leakage currents were subtracted off-line using steps in the range from −120 to −80 mV assuming that all channels are closed at voltages ≤ −80 mV.

Data were analyzed using home-written software (written in Visual C++, Microsoft) and the SigmaPlot program (Jandel Scientific, San Rafael, CA). Noise analysis was performed as described (Pusch, 1998). The frequency dependence of the unitary currents obtained from noise-analysis was analyzed with the following assumptions. If channels undergo a fast flickering process that is independent of the normal slower gating, and if the data traces are filtered at a cutoff frequency f that is well above the frequency corresponding to the normal gating transitions, the nonstationary variance can be approximated by

$$\sigma^2(f) = I*(i + \mathrm{Var_i}(f)/i) - I^2/N,$$

where I is the macroscopic current, N is the number of channels, i is the averaged single-channel current after heavy filtering, and $\mathrm{Var_i}(f)$ is the variance of a single open flickering channel. If the flicker can be described by a simple two-state process with blocking rate, α_B, and unblocking rate, β_B, the averaged single-channel current i is given by

$$i = i_{\mathrm{full}} \frac{\beta_B}{\alpha_B + \beta_B},$$

where i_{full} is the current of the fully open (unblocked) channel, and $Var_i(f)$ is given by

$$Var_i(f) = 2i^2\alpha_B/(\pi\beta_B) * atan(2\pi f/(\alpha_B + \beta_B)).$$

Fitting the (filtered) variance-mean plot with the usual equation,

$$\sigma^2 = I * i_{app} - I^2/N, \quad (1)$$

yields, thus, an estimate of the apparent single-channel current of the form,

$$i_{app}(f) = i * \left(1 + \frac{2\alpha_B}{\pi\beta_B}\,\mathrm{atan}\left(\frac{2\pi f}{\alpha_B + \beta_B}\right)\right). \quad (2)$$

At low frequencies, the flicker is not resolved at all, and i_{app} approaches the lower limit, i. At high frequencies, the flicker is fully resolved and i_{app} approaches the upper limit i_{full}. The transition occurs around the characteristic frequency, $f_B = (\alpha_B + \beta_B)/(2\pi)$. Eq. 2 was fitted to the data shown in Figs. 5 *E* and 10 *E* with the three parameters i, α_B, and β_B.

Reversal potentials were determined from tail current protocols by fitting a parabolic equation to the instantaneous tail currents close to the reversal potential. Liquid junction potentials caused by changing from potassium to rubidium solutions were small (<2 mV) and neglected.

RESULTS

Gating of homomeric KCNQ1 channels in rubidium

We have previously shown that the most interesting features of homomeric KCNQ1 are best seen in tail currents during repolarization in high potassium, although the same features can be observed in normal high sodium solutions (Pusch et al., 1998). Therefore, the currents mediated by homomeric KCNQ1 and heteromeric KCNQ1/KCNE1 channels were recorded in high extracellular potassium or rubidium solutions. In high extracellular potassium, homomeric KCNQ1 currents are characterized by a pronounced hook of the repolarization tail indicative of recovery from an inactivation process that occurred during the depolarizing prepulse (Fig. 1 *A*) (Pusch et al., 1998; Tristani-Firouzi and Sanguinetti, 1998). Exchanging extracellular potassium with rubidium led to a drastic increase of inward tail currents by about threefold (Fig. 1, *B* and *C*), whereas outward tail

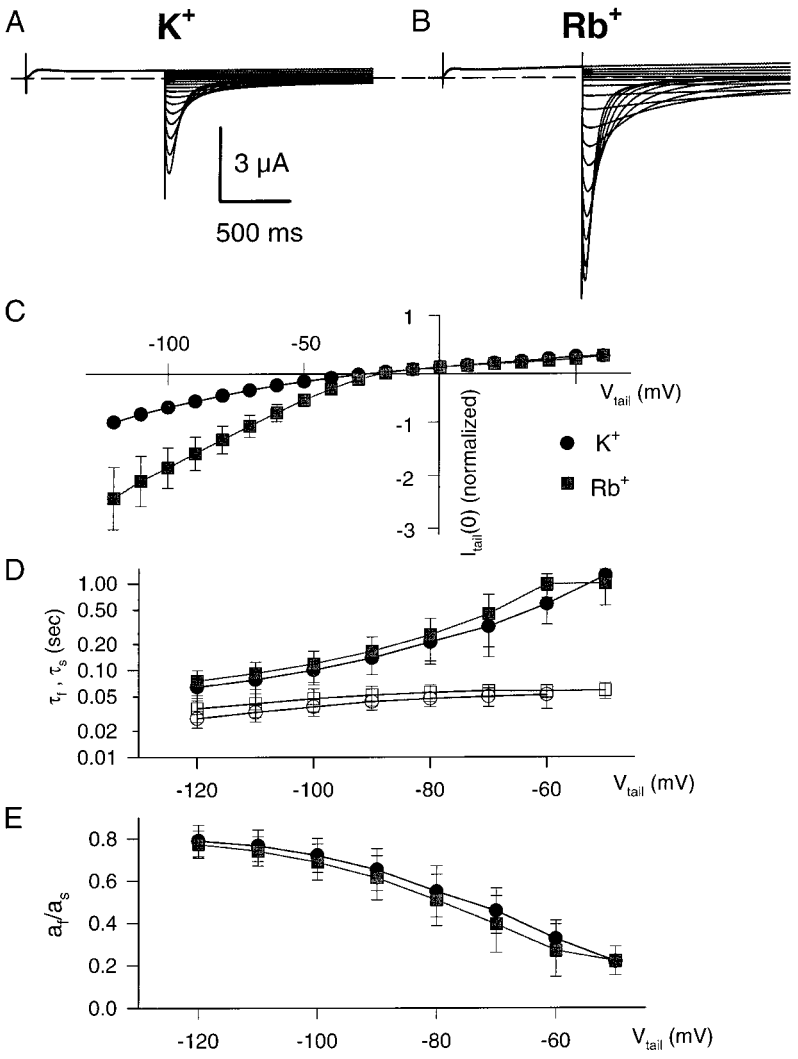

FIGURE 1 Tail currents of homomeric KCNQ1 recorded in (*A*) high potassium (100 K) and (*B*) high rubidium (100 Rb) solutions. Tail currents were elicited after a 1-s prepulse to +40 mV stepping the potential from −120 to +40 mV in 10-mV increments. Traces in (*A*) and (*B*) are from the same oocyte. (*C*) The instantaneous IV in 100 K (*circles*) and 100 Rb (*squares*) obtained from the initial tail current amplitudes normalized to $I_t(-120\ mV)$ in 100 K is shown ($n = 6$, ±SEM). For tail voltages $V_t \leq -50$ mV tail currents were fitted with a biexponential function (+ a constant value) (Eq. 3). (*D*) Mean values of the two time constants (*filled symbols*, slow time constant; *open symbols*, fast time constant) and (*E*) the ratio of the fast and slow component $r = a_f/a_s$ are plotted as a function of V_t.

currents (carried in both cases by potassium) were almost unchanged. Assuming that the number of channels does not change in the presence of rubidium, such an increase of current can be caused either by an increase of the single channel conductance or by an increased open probability. We first examined whether the increased current amplitude in rubidium was accompanied by changes of gating parameters. To this end, tail currents were fitted by a double-exponential function of the form,

$$I(t) = a_s \exp(-t/\tau_s) - a_f \exp(-t/\tau_f) + a_\infty, \qquad (3)$$

with a slow time constant τ_s and a fast time constant τ_f and their respective contributions, a_s and a_f, and a steady-state current, a_∞, that is close to zero at voltages ≤ -60 mV. The larger the fast component, a_f, the more pronounced is the hook of the respective tail current. Tail currents of KCNQ1 in high potassium are well described by such a biexponential function (Pusch et al., 1998). Also, in rubidium, tail currents are well fitted by a double-exponential function. Despite the large increase of the tail current magnitude, the two time constants and the ratio of the fast and slow component, $r = a_f/a_s$, were not grossly affected by rubidium (Fig. 1, *D* and *E*).

The voltage dependence of the steady-state activation of homomeric KCNQ1 was assessed using 2-s conditioning pulses to various voltages, V_p, followed by a repolarizing pulse to -80 mV. Activation probability was estimated as proportional to the initial current, $I(0)$, following the repolarization step (Fig. 2, *A* and *B*). The dependence of $I(0)$ on Vp was fitted with a Boltzmann distribution that gave an adequate fit with the two parameters $V_{1/2}$ (voltage of half-maximal activation) and the slope factor k (see legend to Fig. 2). These parameters have no simple meaning because of the complicated gating of KCNQ1. However, a small effect of rubidium on KCNQ1 gating is revealed by a positive shift of $V_{1/2}$ by about 9 mV (Fig. 2 *C*) without a significant change of the slope factor k (Fig. 2 *D*).

To examine in more detail possible gating effects of rubidium, an envelope of tail currents protocol was used (Pusch et al., 1998). Example traces are shown in Fig. 3 at various voltages. It can be seen that, in rubidium, the characteristic hook of tail currents of homomeric KCNQ1 becomes evident at slightly more negative voltages and that the delay of the hook is slightly less pronounced. The tail currents at -120 mV of the envelope protocol were fitted with a biexponential function (Eq. 3), and the averaged parameters of these fits are shown in Fig. 4 as a function of the duration of the prepulse (t_p) at various prepulse voltages, Vp. It can be seen that, e.g., at 0 mV the delay of inactivation measured as the delay of the ratio a_f/a_s is significantly larger in potassium ($\geq$200 ms) compared to rubidium solutions ($<$100 ms) (compare squares in Fig. 4, *E* and *F*). Apart from a drastic increase of both exponential components, however, their dependence on voltage and duration of the prepulse seems only slightly affected by rubidium.

In conclusion, although rubidium drastically increases absolute inward tail-current amplitude of homomeric

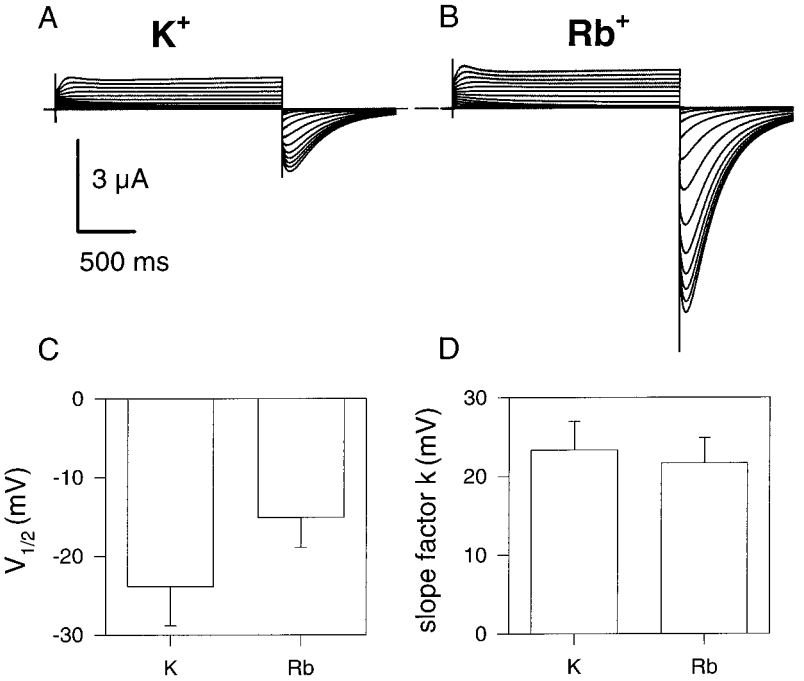

FIGURE 2 Steady-state current–voltage relationship of homomeric KCNQ1 recorded in (*A*) high potassium (100 K) and (*B*) high rubidium (100 Rb) solutions. Traces in (*A*) and (*B*) are from the same oocyte. From the holding potential $V_h = -80$ mV, the voltage was stepped for 2 s to various voltages from $+40$ to -90 mV in 10-mV steps and then returned to -80 mV. Activation was monitored as the initial current following the repolarization and normalized to the maximal current obtained after the most positive prepulses. The resulting steady-state IV was fitted by Boltzmann distribution of the form $f(V) = 1/\{1 + \exp[(V_{1/2} - V)/k]\}$ with two parameters, $V_{1/2}$ (voltage of half-maximal activation) and k (slope factor). Mean values for these two parameters are shown in (*C*) and (*D*), respectively.

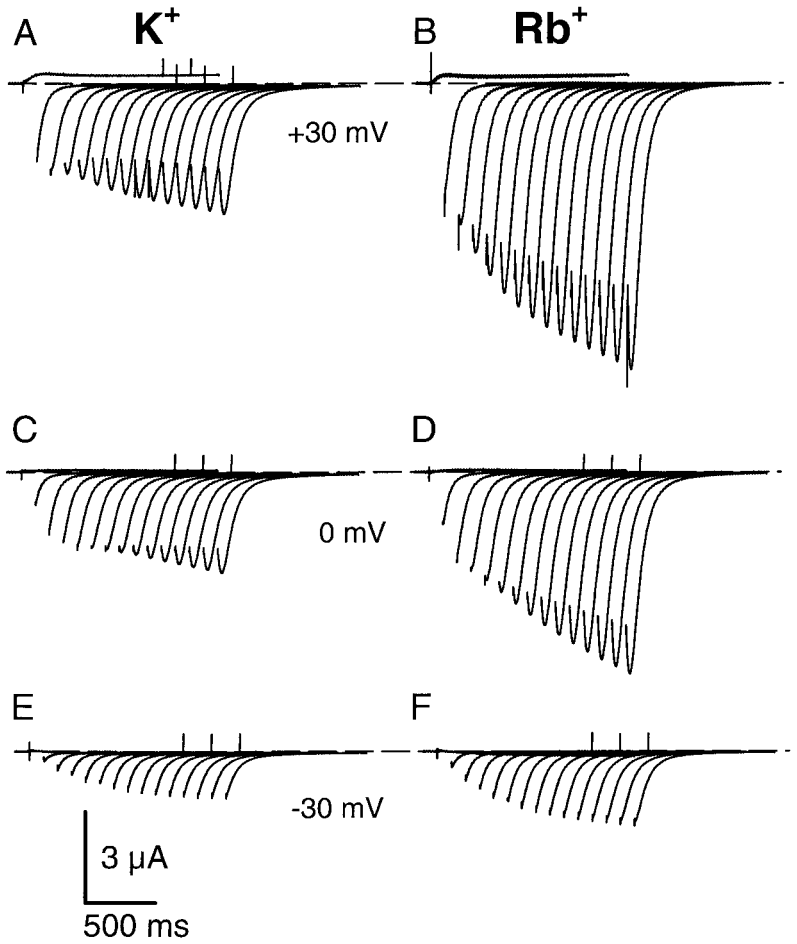

FIGURE 3 Envelope of tail currents of homomeric KCNQ1 recorded in high potassium (100 K) (*left panels*) and high rubidium (100 Rb) (*right panels*) solutions. Tail currents were recorded at −120 mV after prepulses of variable duration (from 1.4 to 0.1 s, shown superimposed in the various panels) and of variable prepulse voltage, V_p. Traces are shown for three different V_p as indicated (recorded from the same oocyte).

KCNQ1, only relatively slight changes of gating parameters are observed.

Relative rubidium-permeability and single-channel current of homomeric KCNQ1 channels in rubidium

From the shift of the reversal potential determined from the tail-current protocol when changing the bathing solution from potassium to rubidium, the relative permeability P_{Rb}/P_K was calculated according to the Goldman–Hodgkin–Katz equation as $P_{Rb}/P_K = 0.80 \pm 0.08$ ($n = 5$, ±SD).

The increase of the instantaneous inward tail currents with only a slight change of outward tail currents (Fig. 1) strongly suggests a change of the (inward) single-channel amplitude. In fact, all the results described above would be easily explained by an increase of the (inward) single-channel current in rubidium. Because single channels are difficult of measure for KCNQ1 (Yang and Sigworth, 1998; Sesti and Goldstein, 1998), we estimated the single-channel amplitude in potassium and rubidium using nonstationary noise analysis of currents recorded from cell-attached patches (Pusch, 1998). When measured at the recording bandwidth of 5 kHz, the averaged single-channel current at −100 mV was about 1.2-fold larger in rubidium compared to potassium ($i = -0.12 \pm 0.03$ pA in potassium [$n = 7$; ±SD] $i = -0.15 \pm 0.04$ pA in rubidium [($n = 11$; ±SD]) (see Fig. 5, *A–D*). This slight increase would not be enough to explain the large difference of the macroscopic inward tail currents. These apparently conflicting results could be explained if the main effect of rubidium was to change an open-channel flicker process by, e.g., favoring the fully open state(s) versus the closed/blocked state(s) without grossly changing the single-channel amplitude of the fully open state(s). To test this hypothesis, we performed the nonstationary noise analysis after digitally filtering the original current traces at various frequencies, f (Fig. 5, *A–D*). The apparent single-channel conductance, γ, decreases with decreasing frequency in both conditions (Fig. 5 *E*) as has also been observed by Yang and Sigworth (1998). γ decreases already at frequencies that are well above the frequencies corresponding to the macroscopic gating relaxations (the fastest macroscopic gating time constant of ≈25 ms corresponds to frequency of less than 10 Hz). The decrease of γ, therefore, indeed indicates the presence of a

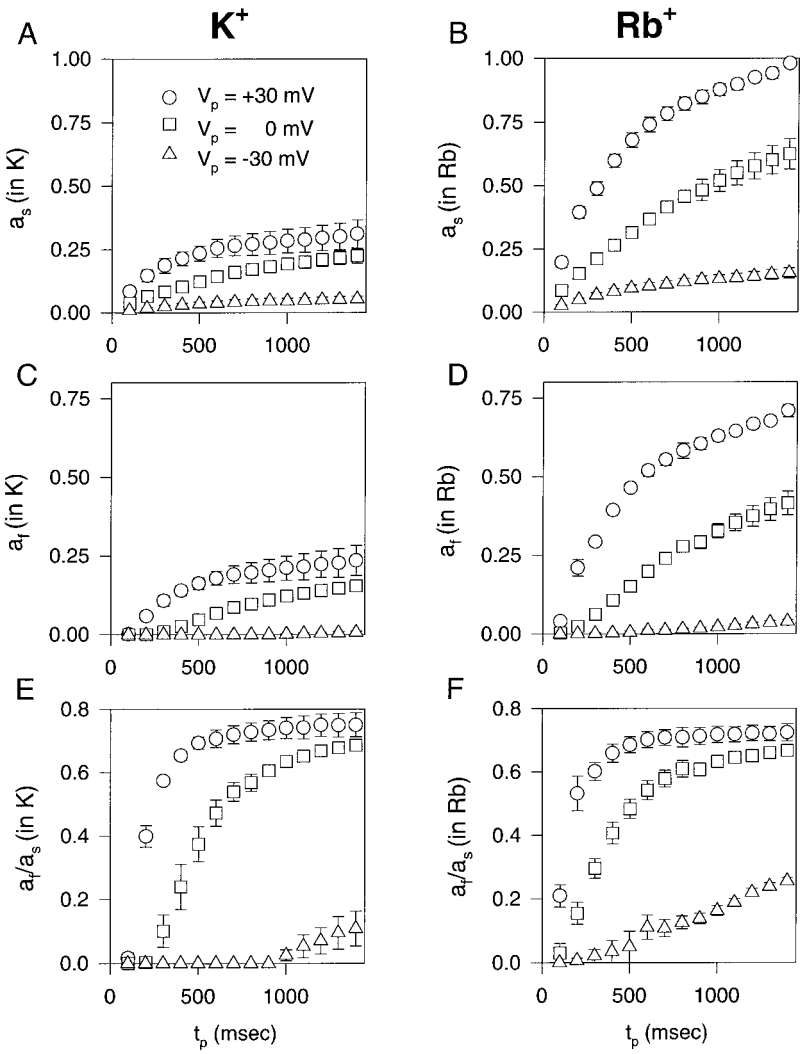

FIGURE 4 Development of slow and fast deactivating components determined from the envelope of tail currents protocol shown in Fig. 3 for homomeric KCNQ1. The tail currents at −120 mV of the envelope protocol were fitted by a double-exponential function (Eq. 3) and the dependence of the two components, (*A* and *B*) a_s and (*C* and *D*) a_f, is plotted as a function of the prepulse-duration, t_p, for various prepulse voltages, V_p, in high potassium (*left panels*) and high rubidium (*right panels*). All coefficients were normalized to the maximal value of as measured in high rubidium after the most positive prepulses, and then averaged ($n = 7$). The ratio of the two exponential components a_f/a_s are shown in (*E*) potassium and (*F*) rubidium.

flickery process. Interestingly, the frequency dependence of γ is different in rubidium such that the ratio of γ in potassium to that in rubidium becomes smaller at lower cutoff frequencies (Fig. 5 *F*), reaching a value around 0.5 at 10 Hz. This suggests that the increase of the instantaneous inward tail currents in rubidium is caused by increase of the apparent single conductance measured at a low bandwidth due to a favoring of a flicker-unblocked state. In case of a flicker block that occurs with on- and off-rate constants, α_B and β_B, respectively, the frequency dependence of the single-channel conductance, γ, estimated by nonstationary noise analysis of time-dependent gating relaxations that occur at much slower rates can be approximated by Eq. 2 (see Methods). Eq. 2 was fitted to the data shown in Fig. 5 *E* with the three parameters, γ, α_B, and β_B (*solid lines* in Fig. 5 *E*). The effect of rubidium is to reduce the occupancy of the flicker blocked state by reducing α_B from 2000 s^{-1} to 820 s^{-1} with almost no change of β_B. The value of the maximal conductance, γ_{full}, is 1.2-fold larger in rubidium.

Gating of heteromeric KCNQ1/KCNE1 channels in rubidium

Heteromeric KCNQ1/KCNE1 channels do not show a significant inactivation when measured in high potassium (Pusch et al., 1998) (Fig. 6 *A*). Replacing extracellular potassium by rubidium led to a reduction of inward tail currents (Fig. 6, *B* and *C*), and, in addition, tail currents showed a strong sigmoidal time course (Fig. 6 *B*). Such a sigmoidicity indicates the presence of several open states and, possibly, a voltage-independent inactivation process similar to that found in homomeric channels. In contrast to homomeric KCNQ1, however, no hook, i.e., no transient increase of the current, was observed under any condition, even at more negative tail voltages (data not shown).

When recorded at a relatively high time resolution, tail currents of heteromeric KCNQ1/KCNE1 channels are slightly sigmoidal also in high potassium (Pusch et al., 1998) (Fig. 6 *A*). Therefore, tail currents were fitted by a

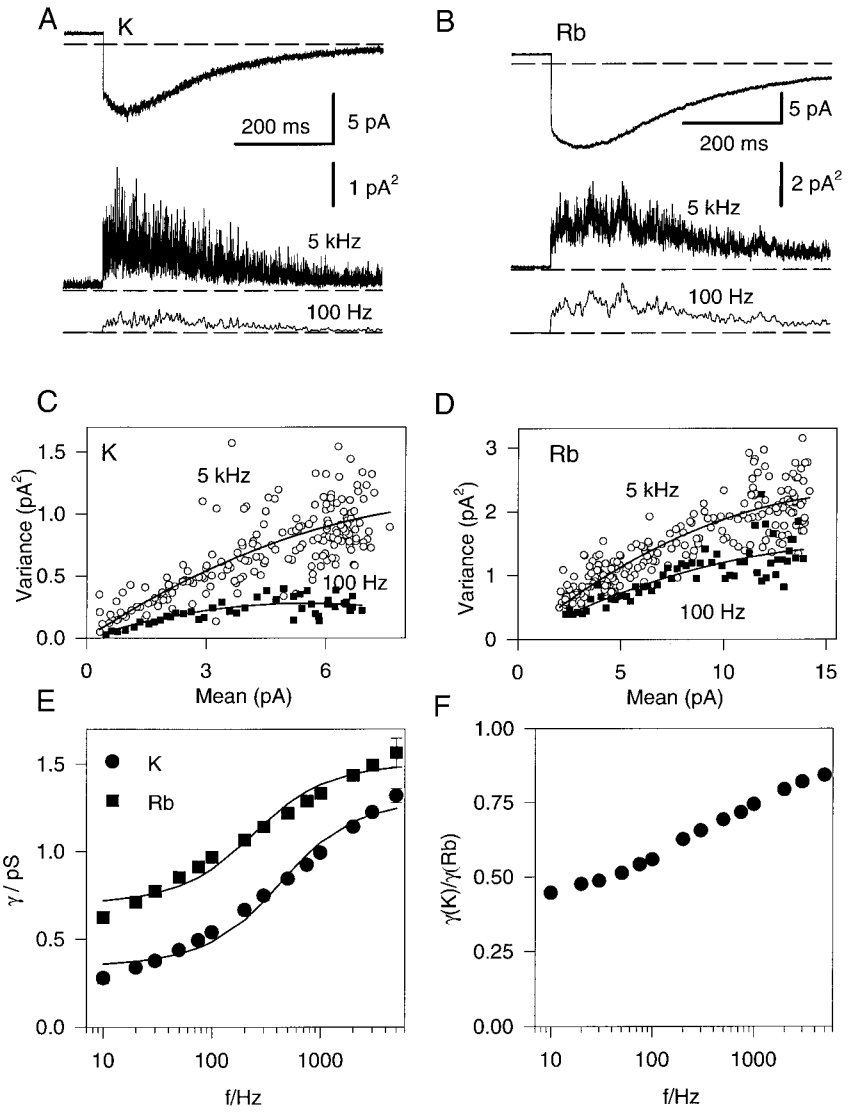

FIGURE 5 Noise analysis of homomeric KCNQ1. Currents were recorded from cell-attached patches with 100 mM of (*A*) potassium or 100 mM (*B*) rubidium in the pipette. Tail currents at −100 mV were evoked after conditioning pulses to +60 mV of 0.6-s duration. Variance and mean of the tail currents were calculated as described (Pusch, 1998). To investigate the frequency dependence of the apparent single channel conductance, the data traces were digitally filtered with a Gaussian filter at various cutoff frequencies, and the noise analysis was performed on the filtered traces. Example traces are shown in *A* (example of a patch measured with potassium in the pipette) and *B* (example for a patch with rubidium in the pipette) for the recording bandwidth (5 kHz) and after filtering at 100 Hz. The mean was not significantly affected by the filtering for frequencies ≥20 Hz. At 10 Hz, also, the mean current was slightly distorted. The corresponding variance mean plots together with the fits to a parabolic equation (Eq. 1) are shown in *C* and *D* (*open circles*, 5 kHz; *filled square*, 100 Hz). Apparent single-channel currents were converted to conductance dividing by −100 mV, and the mean value of several patches was plotted versus the cutoff frequency (*E*) *Circles*, potassium ($n = 7$); *squares*, rubidium ($n = 11$); error bars indicate SEM. The solid lines are fits of Eq. 2 with the three parameters γ, α_B, and β_B (γ corresponds to i in Eq. 2, the minimal single-channel current measured after heavy filtering). The values obtained are: potassium, $\gamma = 0.35$ pS, $\alpha_B = 2000\ s^{-1}$, $\beta_B = 720\ s^{-1}$; rubidium, $\gamma = 0.70$ pS, $\alpha_B = 820\ s^{-1}$, $\beta_B = 710\ s^{-1}$. From these values, the fully open conductance can be calculated as $\gamma_{full} = 1.3$ pS in potassium and $\gamma_{full} = 1.5$ pS in rubidium. (*F*) The ratio of the conductance in potassium to that in rubidium is plotted as a function of the cutoff frequency.

similar double exponential function used for homomeric channels (Eq. 3). Tail currents at voltages ≤ −40 mV are well fitted by such a function in potassium and rubidium solutions.

The slow time constant, τ_s, increases monotonically with the tail voltage, V_t, from 0.32 s at −120 mV to ~1.2 s at −50 mV and is not grossly affected by rubidium (Fig. 6 *D*). In contrast, the fast time constant, τ_f, decreases slightly with V_t and is significantly increased at all voltages V_t and is less voltage dependent in rubidium compared to potassium (*open symbols* in Fig. 6 *D*).

The more sigmoidal time course of heteromeric tail currents in rubidium compared to potassium is especially evident as an increased ratio of the fast and slow component, $r = a_f/a_s$ (Fig. 6 *E*). The ratio a_f/a_s decreases at tail voltages more positive than −120 mV in a similar manner found for homomeric channels (compare Figs. 1 *E* and 6 *E*), suggesting that a similar mechanism may underlie the sigmoidal deactivation in heteromeric channels and the hook of tail currents in homomeric channels.

When measured in two-electrode voltage clamp, heteromeric KCNQ1/KCNE1 channels do not reach steady state even after pulses as long as 100 sec (data not shown). To investigate effects of rubidium on the voltage dependence of steady-state activation, we restricted ourselves to pulse protocols with 10-s duration and fitted the resulting current–voltage relationship (IV) with a Boltzmann distribution (Fig. 7). It can be seen that rubidium has only a small effect on the resulting parameters of the Boltzmann fit, i.e., the voltage of half-maximal activation, $V_{1/2}$, and the slope factor, k.

To investigate the sigmoidal deactivation in more detail, we applied an envelope of tail-currents protocol similar to that used for homomeric channels, but with longer pulse durations (Fig. 8). Because of the relatively long total durations of the pulse protocols, we restricted ourselves to

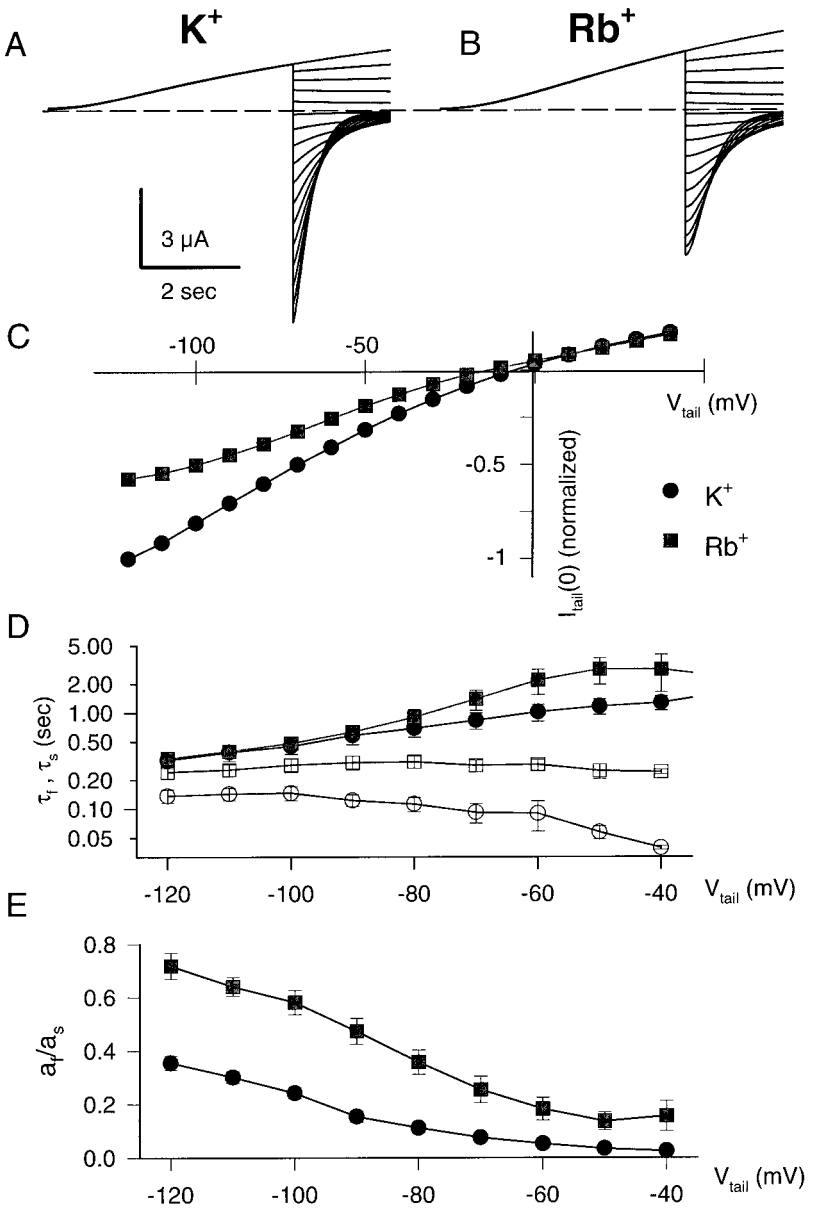

FIGURE 6 Tail currents of heteromeric KCNQ1/KCNE1 recorded in (*A*) high potassium (100 K) and (*B*) high rubidium (100 Rb) solutions. Tail currents were elicited after a 5-s prepulse to +40 mV stepping the potential from −120 to +40 mV in 10-mV increments. Traces in (*A*) and (*B*) are from the same oocyte. (*C*) The instantaneous IV in 100 K (*circles*) and 100 Rb (*squares*) obtained from the initial tail current amplitudes normalized to $I_t(-120\ \text{mV})$ in 100 K is shown ($n = 5$, ±SEM; error bars are smaller than symbols). For tail voltages $V_t \leq -40$ mV, tail currents were fitted with a biexponential function (+ a constant value) (Eq. 3). Mean values of (*D*) the two time constants (*filled symbols*, slow time constant; *open symbols*, fast time constant) and (*E*) the ratio of the fast and slow component $r = a_f/a_s$ are plotted as a function of V_t. At voltages $V_t \leq -100$ mV, the two time constants were relatively close, especially in high potassium, rendering the fitting procedure less stable than for homomeric channels.

conditioning potentials of +40, +20, and 0 mV and conditioning pulse durations of 6 s and less. The tail potential was chosen as −100 mV because, on one hand, the sigmoidicity is significantly pronounced at this potential (Fig. 6, *B* and *E*), and on the other hand, when fitted by a double-exponential function, the two-tail time constants are sufficiently distinct (Fig. 6 *D*). The time constants were relatively independent of prepulse voltage and duration. Qualitatively similar to homomeric channels, the ratio $r = a_f/a_s$ developed with a significant delay (≈2 s at 0 mV in high potassium, Fig. 9 *E*). The delay is significantly reduced in rubidium (<1.5 s at 0 mV, Fig. 9 *F*). Interestingly, the ratio a_f/a_s seems to reach almost a steady state at all voltages tested after the 6-s conditioning prepulse (Fig. 9, *E* and *F*), whereas both a_s and a_f continue to increase (Fig. 9, *A–D*). Another interesting feature emerging from this analysis is that, although the initial tail current is decreased in high rubidium, both the slow and the fast component are increased in rubidium similar to the situation seen for homomeric channels. The reduction of the initial tail current is reflected predominantly as an increase of the fast component, a_f.

Relative rubidium permeability and single-channel current of heteromeric KCNQ1/KCNE1 channels in rubidium

From the shift of the reversal potential when changing the bathing solution from potassium to rubidium, the relative

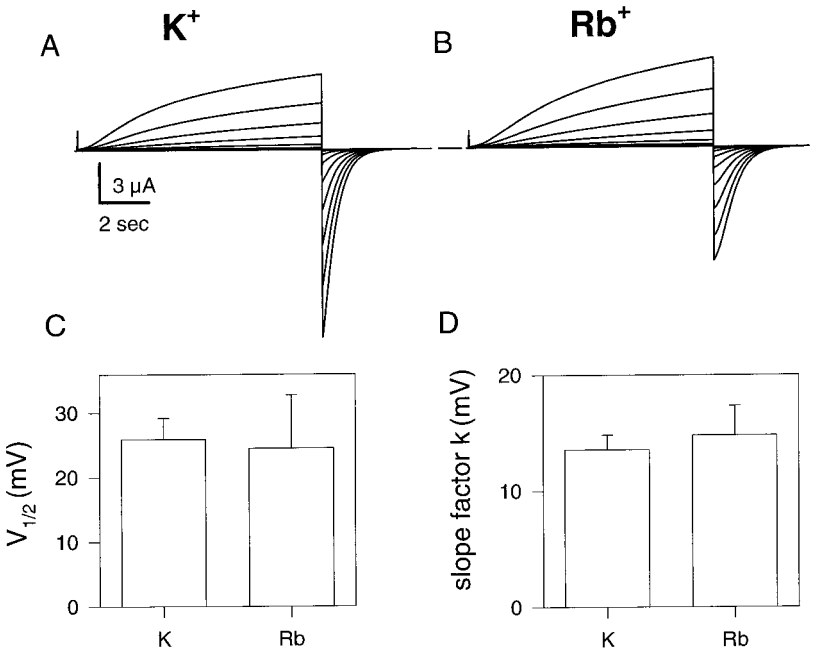

FIGURE 7 Steady-state current–voltage relationship of heteromeric KCNQ1/KCNE1 recorded in (*A*) high potassium (100 K) and (*B*) high rubidium (100 Rb) solutions. Traces in (*A*) and (*B*) are from the same oocyte. From the holding potential $V_h = -80$ mV, the voltage was stepped for 10 s to various voltages from +40 to −90 mV in 10-mV steps and then returned to −80 mV. Activation was monitored as the initial current following the repolarization and normalized to the maximal current obtained after the most positive prepulses. The resulting steady-state IV was fitted by Boltzmann distribution of the form $f(V) = 1/\{1 + \exp[(V_{1/2} - V)/k]\}$ with two parameters: (*C*) $V_{1/2}$ (voltage of half-maximal activation) and (*D*) k (slope factor).

permeability, P_{Rb}/P_K, was calculated as $P_{Rb}/P_K = 0.78 \pm 0.05$ ($n = 6$, ±SD) not significantly different from homomeric KCNQ1.

The single-channel current of heteromers in potassium and rubidium was estimated using nonstationary noise analysis of currents recorded from cell-attached patches by repeatedly applying voltage steps to −120 mV from a positive holding potential (Pusch, 1998). In contrast to homomeric KCNQ1, the averaged single-channel current was reduced significantly by about twofold in rubidium compared to potassium ($i = 0.83 \pm 0.2$ pA in potassium]$n = 6$; ± SD[$i = -0.45 \pm 0.12$ pA in rubidium [$n = 10$; ± SD]) (Fig. 10, *A–D*) when measured at a 5-kHz bandwidth. This decrease of the single channel current parallels the decrease of the macroscopic inward tail currents. Similar to homomers, γ was decreased when the noise analysis was performed on filtered data (Fig. 10, *A–E*), demonstrating that a similar flicker-block is present in heteromers. The solid lines in Fig. 10 *E* correspond to a fit of Eq. 2 with the parameters given in the legend. Rubidium changes only slightly the blocking/unblocking rates α_B and β_B and the flicker-block probability. The main effect is a reduction of the fully open conductance from 7.6 pS in potassium to 3.8 pS in rubidium. The relative decrease of γ in rubidium is almost independent of the cutoff frequency used for the analysis (Fig. 10 *F*).

Concentration dependence of the rubidium effects in homomeric KCNQ1 and heteromeric KCNQ1/KCNE1

To get further insight into the mechanism of the effects of rubidium on homomeric and heteromeric channels, the concentration of external cations was varied in whole-oocyte voltage-clamp recordings. We first tested the idea that the fast flickering process might be related to a block of the channels by external divalent cations. Our usual recording solution contained 0.5 mM calcium and 3 mM magnesium. We could not remove all divalent cations from the external solution because this invariably caused a large unspecific increase in the membrane conductance. However, external solutions with only 1 mM magnesium as divalent ion showed no significant effect on current magnitude or kinetics, neither for homomeric KCNQ1 (tail currents increased by less than 2% in solutions with only 1 mM magnesium [$n = 6$ oocytes]) nor for heteromeric KCNQ1/KCNE1 (tail currents increased by less than 6% in solutions with only 1 mM magnesium [$n = 4$ oocytes]) channels (data not shown). The flickering process thus seems to be unrelated to divalent cations.

We next tested whether other monovalent cations significantly alter the flickering process. We started recordings in solutions containing only 50 mM potassium or 50 mM rubidium as permeant ions and 100 mM sucrose to compensate for the osmolarity and studied the effect of exchanging sucrose with either 50 mM NaCl, 50 mM CsCl, or 50 mM *N*-methyl-D-glucamine-Cl (NMDG-Cl). Currents in the presence of NMDG or sodium were only slightly different from those measured in sucrose ($n = 3$ oocytes for homomers and $n = 5$ oocytes for heteromers; data not shown), whereas addition of cesium reduced currents under all conditions (block by about 50% in homomers and by about 90% in heteromers; $n = 2$ oocytes for each channel type, data not shown). This blocking effect of cesium is probably at least in part caused by an open channel block that is unrelated to the flickering process, making any quantitative

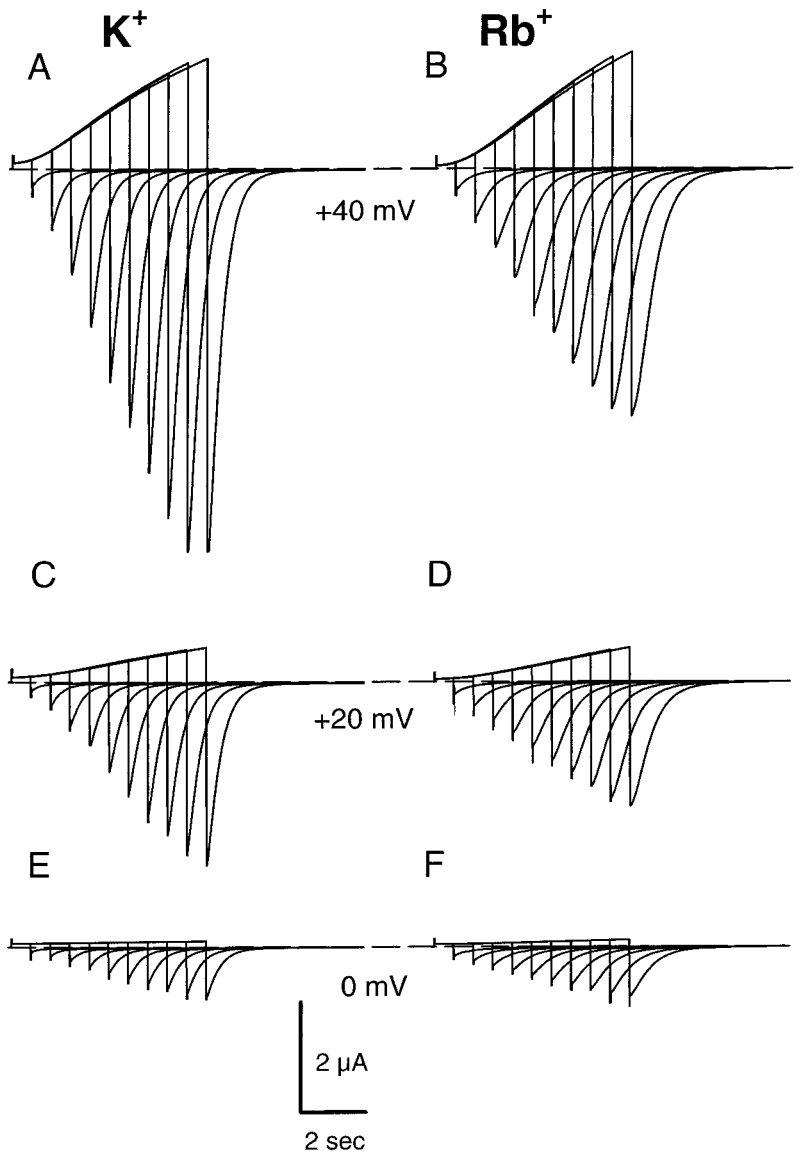

FIGURE 8 Envelope of tail currents of heteromeric KCNQ1/KCNE1 recorded in high potassium (100 K) (*left panels*) and high rubidium (100 Rb) (*right panels*) solutions. Tail currents were recorded at −100 mV after prepulses of variable duration (from 6 to 0.6 s, shown superimposed in the various panels) and of variable prepulse voltage, V_p. Traces are shown for three different V_p as indicated (recorded from the same oocyte).

analysis difficult. The lack of effect of sodium and NMDG on inward tail currents in the presence of 50 mM potassium or rubidium indicates that these ions are unable to interfere with the binding of potassium or rubidium to the site relevant for the flickering process.

We also tested the effect of reducing the external potassium or rubidium concentration from 100 to 50 mM, by exchanging either with 50 mM NMDG-Cl or 100 mM sucrose. Examples for instantaneous current–voltage relationships are shown in Fig. 11 for homomeric KCNQ1 (Fig. 11 *A*) and heteromeric KCNQ1/KCNE1 channels (Fig. 11 *B*). It can be seen that, for both channel types, reduction of the external monovalent cation concentration reduces inward tail currents by slightly less than 50%. This reduction is expected purely on the basis of a reduction of open-channel conductance due to the reduction of permeant ion concentration if it is assumed that the single channel conductance saturates at much higher potassium concentrations, as is the case, e.g., for squid giant axon potassium channels (Wagoner and Oxford, 1987), *Shaker* potassium channels (Heginbotham and MacKinnon, 1993), and sugar beet tonoplast potassium channels (Gambale et al., 1996). Thus, it appears that the dissociation constant for potassium or rubidium binding to the site responsible for the flickering is much lower than 50 mM, because, otherwise, a change of the occupancy of the flicker-modulatory binding site would be expected to lead to a larger relative change in the current amplitude.

We next investigated in detail the dependence of peak inward tail currents on the relative rubidium concentration by using mixtures of rubidium and potassium, keeping the sum of rubidium and potassium constant at 100 mM. Average results are shown in Fig. 12 for homomers (*circles*) and heteromers (*squares*). The concentration dependence is

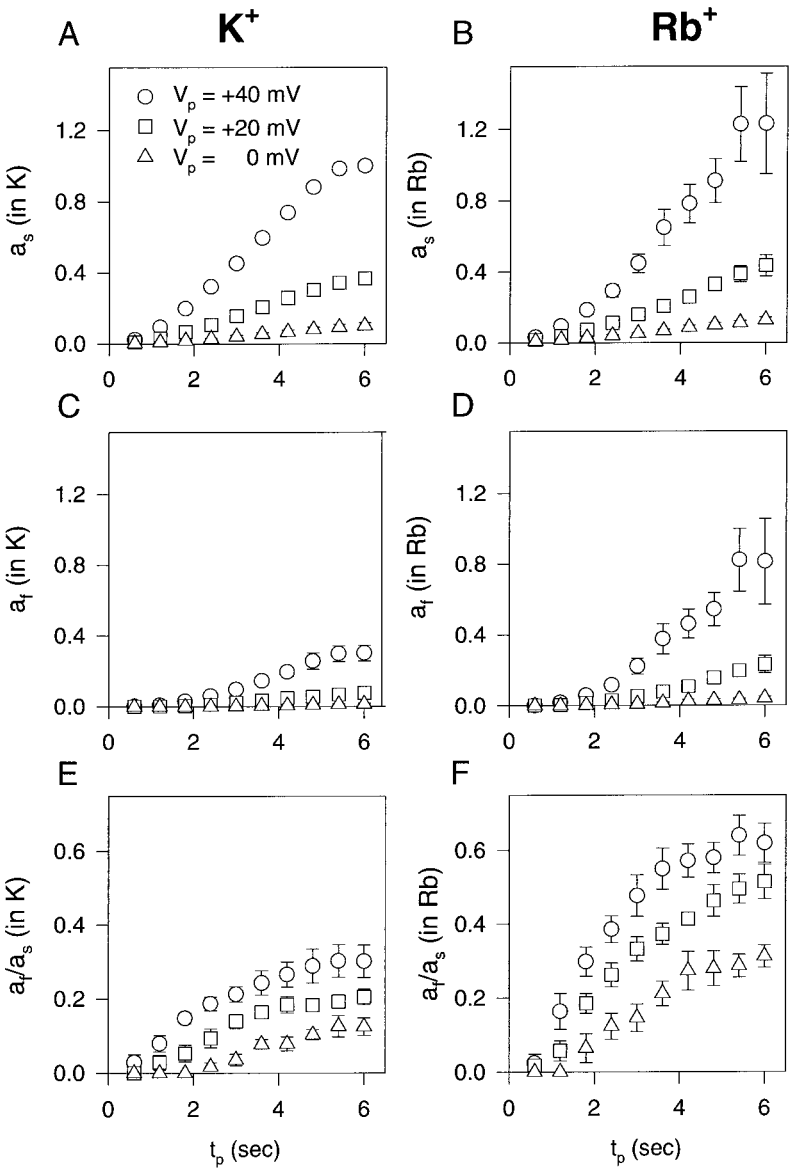

FIGURE 9 Development of slow and fast deactivating components determined from the envelope of tail currents protocol shown in Fig. 8 for heteromeric KCNQ1/KCNE1. The tail currents at −100 mV of the envelope protocol were fitted by a double-exponential function (Eq. 3), and the dependence of the two components, (*A* and *B*) a_s and (*C* and *D*) a_f, is plotted as a function of the prepulse duration, t_p, for various prepulse voltages, V_p, in high potassium (*left panels*) and high rubidium (*right panels*). All coefficients were normalized to the maximal value of as measured in high potassium after the most positive prepulses, and then averaged ($n = 6$). The ratio of the two exponential components a_f/a_s in (*E*) potassium and (*F*) rubidium.

clearly different for the two channel types: homomeric channels are almost unaffected by rubidium at concentrations below 50 mM and increase then steeply without saturation at higher fractional rubidium content. Currents through heteromeric channels, in contrast, decrease already at 10 mM rubidium and reach a plateau at 50 mM rubidium. This result further strengthens the conclusion that association of KCNQ1 with KCNE1 drastically alters the impact of external rubidium on the channel properties.

DISCUSSION

In this paper, we have analyzed gating and conduction of homomeric KCNQ1 and heteromeric KCNQ1/KCNE1 channels in high rubidium and potassium solutions. We found that rubidium has quite different effects on the properties of these two channel complexes. Although inward tail currents of homomeric channels are drastically increased with only little changes of gating parameters, tail currents of heteromeric channels are decreased and become significantly sigmoidal. Noise analysis indicated that rubidium has only slight effects on the single-channel current of homomeric channels when measured at a 5-kHz bandwidth. However, the apparent conductance is strongly dependent on the cutoff frequency and the apparent conductance is significantly larger in rubidium compared to potassium at lower cutoff frequencies. In contrast, in heteromeric KCNQ1/KCNE1 channels, the apparent single-channel current in rubidium is significantly reduced independent of the bandwidth, and the reduction is the same as that of the macroscopic inward tail currents.

A pronounced frequency dependence of γ at frequencies well above those corresponding to macroscopic gating relaxations has also been reported by Yang and Sigworth

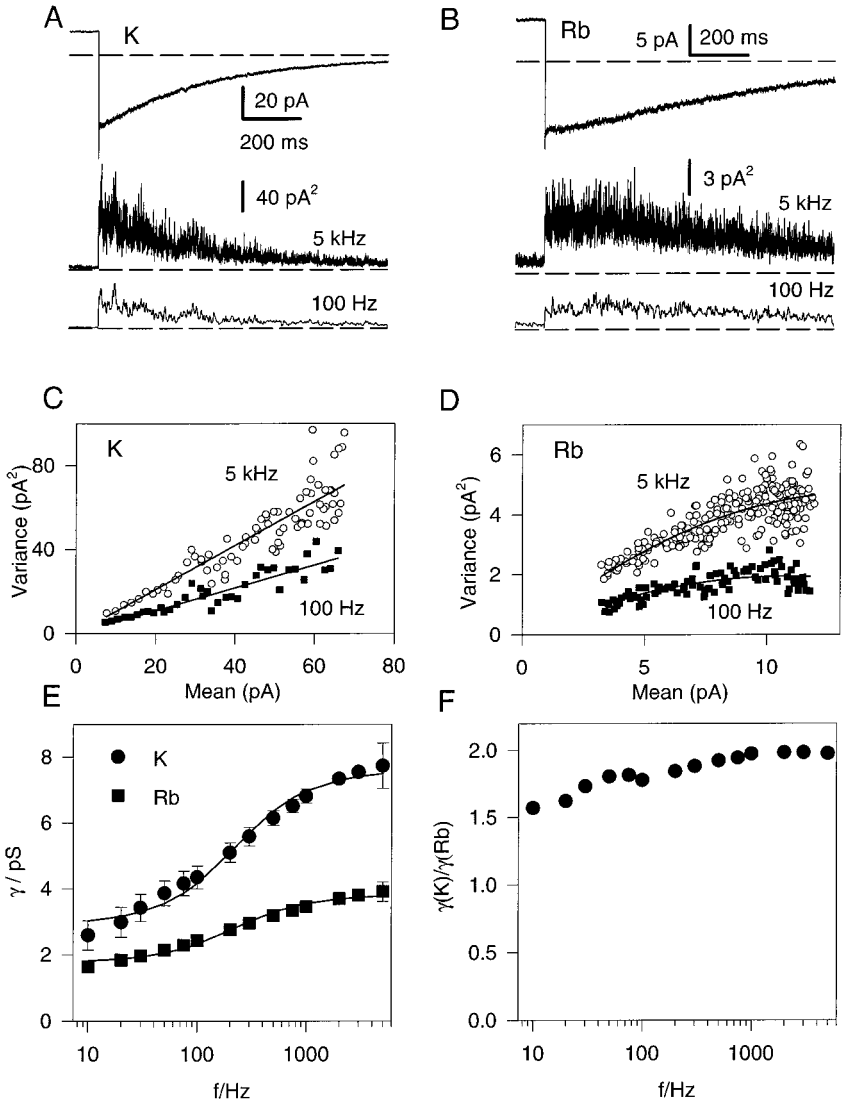

FIGURE 10 Noise analysis of heteromeric KCNQ1/KCNE1. Currents were recorded from cell-attached patches with 100 mM potassium or 100 mM rubidium in the pipette. Tail currents at −120 mV were evoked from a positive holding potential. Analysis was performed as for homomers (Fig. 5). Example traces are shown in *A* (example of a patch measured with potassium in the pipette) and *B* (example for a patch with rubidium in the pipette) for the recording bandwidth (5 kHz) and after filtering at 100 Hz. The corresponding variance mean plots, together with the fits to a parabolic equation (Eq. 1) are shown in *C* and *D* (*open circles*, 5 kHz; *filled squares*, 100 Hz). (*E*) Apparent single-channel currents were converted to conductance dividing by −120 mV, and the mean value was plotted versus the cutoff frequency of the digital Gaussian filter (*circles*, potassium (n = 6); *squares*, Rb (n = 10); error bars indicate SEM). The solid lines are fits of Eq. 2 with the three parameters γ, α_B, and β_B (γ corresponds to i in Eq. 2). The values obtained are: potassium: γ = 2.9 pS, α_B = 870 s^{-1}, β_B = 530 s^{-1}; rubriumRb: γ = 1.8 pS, α_B = 730 s^{-1}, β_B = 620 s^{-1}. From these values, the fully open conductance can be calculated as γ_{full} = 7.6 pS in potassium and γ_{full} = 3.8 pS in rubidium. (*F*) The ratio of the conductance in potassium to that in rubidium is plotted as a function of the cutoff frequency.

(1998) and Sesti and Goldstein (1998), and it indicates the presence of a fast flicker process. This flicker seems not to be responsible per se for the conductance difference of homomeric and heteromeric channels (Sesti and Goldstein, 1998). Here, we find that the flicker is influenced by external rubidium in homomeric KCNQ1: rubidium decreases the probability of the channel to be in the flicker-blocked state, thereby increasing the mean single-channel conductance and causing an increase of the macroscopic inward tail currents. We find that the true single-channel conductance of homomers is about equal in rubidium and potassium. This conclusion is based on the assumption that the frequency dependence of γ saturates at frequencies ≥5 kHz (see Fig. 5). Yang and Sigworth (1998) did not observe a saturation of the apparent single-channel conductance for frequencies up to 20 kHz, even though γ was measured under quite different conditions. From the data in Fig. 5, it appears that, at higher frequencies, γ_K might indeed tend to become as large as γ_{Rb} and maybe even larger, similar to heteromers. If this were the case, the increase of macroscopic currents in rubidium would imply an even stronger reduction of the flicker-block probability. In contrast, the kinetics and voltage-dependence of macroscopic currents carried by homomeric KCNQ1 channels are only slightly affected by rubidium. This demonstrates that homomeric channels flicker with a similar flicker-block probability also in closed and inactivated states, because, otherwise, the effective rate-constants for transitions leaving the open state(s) would be increased in rubidium by about the same amount as the mean single-channel current, and the current decay would be consequently accelerated. Therefore, the cation binding site responsible for the flicker modulation is most likely located in the extracellular vestibule of the channel and not deeply in the pore. Several mechanisms can be envisioned for such a flicker process. A simple blocking mechanism is inconsistent with the block being most effec-

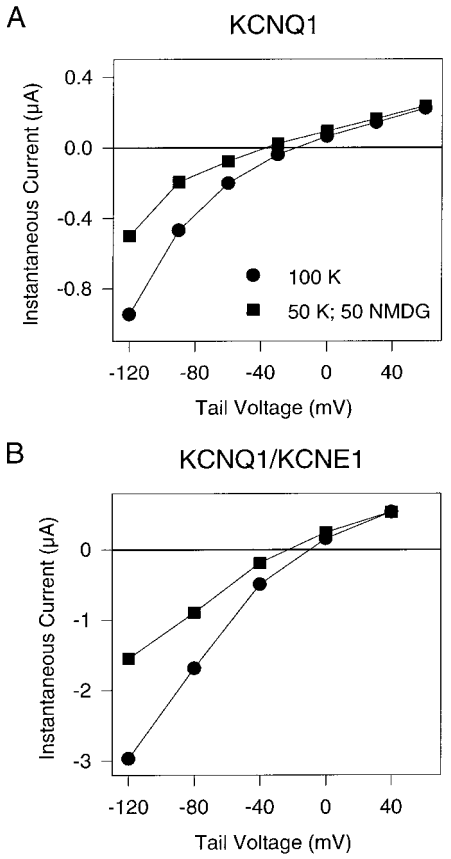

FIGURE 11 Tail currents in 100 mM potassium and 50 mM potassium. Tail currents were evoked after (*A*) 0.5 s (homomeric KCNQ1) or (*B*) 5 s (heteromeric KCNQ1/KCNE1) prepulses to +40 mV, and the instantaneous currents are plotted versus the tail-potential. Oocytes were first bathed in the standard 100 mM KCl external solution (*circles*). Then, 50 mM potassium was replaced by NMDG (*squares*). Shown are representative experiments from one oocyte for each channel type. Similar results were obtained for a total of three oocytes expressing homomeric KCNQ1 and five oocytes expressing heteromeric KCNQ1/KCNE1.

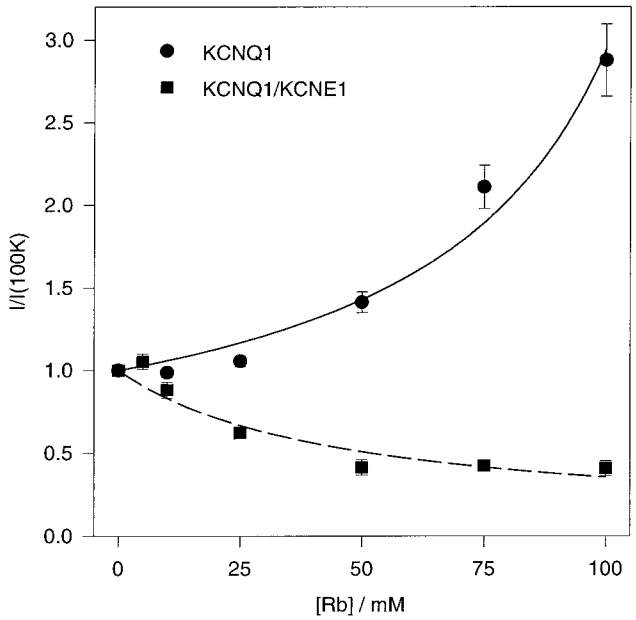

FIGURE 12 Mole fraction behavior in mixtures of potassium and rubidium. Tail currents in mixtures of potassium and rubidium (total concentration: 100 mM) were evoked after 0.5 s (homomeric KCNQ1, *circles*) or 5 s (heteromeric KCNQ1/KCNE1, *squares*) prepulses to +40 mV and the instantaneous current at a tail potential of −120 mV was normalized to the value measured in 100 mM and plotted against the rubidium concentration. Average values from five oocytes are shown for each channel type (error bars are SEM). The solid line is a fit of Eq. 6 to the data for homomeric channels with the parameters given in the text. The dashed line is a fit of the data for heteromeric channels assuming a conductance, γ, that is the algebraic sum of the potassium conductance, γ_K, and the rubidium conductance, γ_{Rb}, assuming that these are simple saturable functions of the competitive binding of potassium and rubidium with affinities A_K and A_{Rb}, respectively, i.e., $\gamma = (\gamma_K[K]A_K + \gamma_{Rb}[Rb]\,A_{Rb})/(1 + [K]A_K + [Rb]A_{Rb})$. The fit yields $A_{Rb} \approx 3 * A_K$ and $\gamma_K \approx 2.8\ \gamma_{Rb}$.

tive by the most permeant ion (potassium) at high concentrations that saturate the pore conductance. We also excluded the idea that the flicker represents a fast block by external divalent cations. A more plausible mechanism may be a protein-intrinsic fast gating process that is modulated by the binding of potassium or rubidium to the gating structure.

To compare the results of the noise analysis with the results of the macroscopic mole-fraction experiments (Fig. 12) we modeled the flicker block with the following simple scheme:

$$\begin{array}{ccccc} U_K & \leftrightarrow & U_0 & \leftrightarrow & U_{Rb} \\ \Downarrow\Uparrow & & \Downarrow\Uparrow & & \Downarrow\Uparrow \\ B_K & & B_0 & & B_{Rb} \end{array}$$

where U denotes unblocked, i.e., open channels, B denotes blocked channel, and the subscript indicates whether the relevant binding site is free (0) or occupied by potassium or rubidium (for simplicity, no communication is allowed among the blocked states as if the cation binding site masked the blocked conformation; for the steady-state calculations, this does not represent a significant restriction). The unblocked states can be assumed to be in rapid equilibrium with relative probabilities $p_0 = 1/(1 + [Rb] * A_{Rb} + [K] * A_K)$, $p_K = [K] * A_K * p_0$, $p_{Rb} = [Rb] * A_{Rb} * p_0$ with the affinities A_K and A_{Rb} for potassium and rubidium, respectively (for convenience, in this and in the following equations, concentrations are measured in units of 100 mM, i.e., an affinity of 1 corresponds to a dissociation constant of 100 mM). The probability to be in any one of the unblocked states can be expressed as

$$p_U = \frac{1 + [Rb]A_{Rb} + [K]A_K}{1/p_U^0 + [Rb]A_{Rb}/p_U^{Rb} + [K]A_K/p_U^K}, \qquad (4)$$

where p_U^0, p_U^{Rb}, and p_{UK} denote the unblock probability of the unoccupied channel, of the channel occupied by rubidium, and of the channel occupied by potassium, respectively

(if the blocking/unblocking rate constants are α and β, respectively, $p_U = \beta/(\alpha + \beta)$).

In the presence of only potassium at 100 mM or 50 mM, the expressions for p_U are reduced to

$$[K] = 100\ mM: \quad p_U = \frac{1 + A_K}{1/p_U^0 + A_K/p_U^K};$$
$$[K] = 50\ mM: \quad p_U = \frac{1 + A_K/2}{1/p_U^0 + A_K/2p_U^K}. \tag{5}$$

In the mole fraction experiments (Fig. 12), the normalized current plotted as a function of the fractional rubidium concentration is proportional to this quantity, p_U. If we assume, for simplicity and in accordance with the results of the noise analysis, that, for homomeric KCNQ1, the single-channel current is not significantly different in rubidium and potassium, using Eq. 4, the normalized current can be expressed as a simple function of the mole fraction of rubidium, x.

$$I_{Norm} = \frac{p_U}{p_U(x = 0)} = \frac{1 + ax}{1 + bx}, \tag{6}$$

with two numbers, a and b, that depend on the parameters of the model:

$$a = \frac{A_{Rb} - A_K}{1 + A_K} \tag{7}$$

$$b = \frac{A_{Rb}/p_U^{Rb} - A_K/p_U^K}{1/p_U^0 + A_K/p_U^K}. \tag{8}$$

A fit of Eq. 6 to the data of Fig. 12 for homomeric KCNQ1 yielded the solid line shown in Fig. 12. The data are reasonably fitted and the fit yielded the values $a = -0.16$ and $b = -0.72$. From these numbers, the parameters of the model are not uniquely determined. Nevertheless, some conclusions can be drawn. First of all, $a < 0$ implies that the affinity of the site for rubidium, A_{Rb}, is smaller than that for potassium, A_K, even though the small absolute value of a indicates that the difference is small. Because the difference of A_K and A_{Rb} is small, $b < 0$ implies that $p_U^{Rb} > p_U^K$, i.e., the blocking probability is larger when the channel is occupied by potassium compared to rubidium. More quantitative conclusions can be drawn if it is assumed that both affinities are much larger than 1 (i.e., the corresponding dissociation constants are much smaller than 100 mM). The experimental finding that a reduction of the external potassium or rubidium concentration from 100 to 50 mM reduces tail currents by about 50% (see Fig. 11) supports this assumption based on the following argument: if we assume that the single channel conductance saturates at much higher potassium concentrations than 50 mM, as in other potassium channels (e.g., Wagoner and Oxford, 1987; Heginbotham and MacKinnon, 1993; Gambale et al., 1996), a reduction of tail currents by about 50% simply reflects the linear dependence of the single channel conductance on concentration. This implies that the unblock probability, that, in turn, depends on the occupancy of the flicker-modulatory binding site, does not change significantly when changing the concentration from 100 to 50 mM, and thus, that this flicker-modulatory site is of high affinity. We have no experimental evidence supporting the assumption of a linear potassium (or rubidium) concentration dependence of the conductance; it is, however, likely that the apparent dissociation constant for the concentration dependence of the conductance is at least several tens of mM, such that the above assumption is still approximately valid.

With this assumption, it follows that $A_{Rb} = 0.84\ A_K$, i.e., the affinity for rubidium is about 80% of that for potassium. As outlined above, the probability of the channels to be in the unblocked state, p_U, does not change significantly by reducing [K] from 100 to 50 mM, and, according to Eq. 5, this is possible only if $1/p_U^0 \ll A_K/p_U^K$. If it can thus be further assumed that the term $1/p_U^0$ in the denominator of Eq. 8 can be neglected, and it follows that $p_U^K/p_U^{Rb} = 0.34$, and, therefore, also $p_B^K = 0.66 + 0.34 * p_B^{Rb}$ (where $p_B^K = 1 - p_U^K$ and correspondingly for rubidium). This means that the blocking probability is at least 0.66 for channels occupied by potassium. These values can be compared with those obtained from the noise analysis (Fig. 5): from the values for α_B and β_B for potassium and rubidium, the following values can be calculated, $p_U^K = 0.26$, $p_B^K = 0.74$, $p_U^{Rb} = 0.46$, $p_B^{Rb} = 0.54$, and $p_U^K/p_U^{Rb} = 0.57$. This value of p_U^K/p_U^{Rb} is in qualitative accordance with that found above from the macroscopic mole-fraction experiments. The largest uncertainties in these quantitative considerations are probably associated with the exact values of the blocking/unblocking rate constants derived from the noise analysis. As discussed above, the frequency dependence of the single channel conductance may not have reached saturation at 5 kHz, in agreement with the findings of Yang and Sigworth (1998), who found an apparent increase of γ even up to 20 kHz. Therefore, the values of α_B and β_B could well be underestimated. Qualitatively, the two types of analysis, noise-analysis and macroscopic mole-fraction dependence, give a similar picture of the process, but more experiments are needed to define the mechanism of flicker in more detail.

We observed a very similar flicker also in heteromeric channels (Fig. 10), but, unlike that of homomeric KCNQ1, this flicker was almost independent of the external cation. This result suggests than KCNE1 interacts with the extracellular vestibule of the channel and thereby alters the properties of the flicker. We can speculate that complexation of KCNQ1 with KCNE1 hinders the binding of external cations to the modulatory site. Accordingly, we would expect a reduction of the positive charge density in the pore vestibule with a consequent increase in the local cation concentration that could contribute to the observed larger single-channel conductance of heteromers, at least for inward currents. The results of the macroscopic mole-frac-

tion experiments (Fig. 12) for heteromeric channels are qualitatively different from those obtained for homomers. Currents decrease to a plateau of about 50% already at relatively low rubidium concentrations. In view of the results from the noise analysis, that showed an approximately twofold smaller single-channel conductance in rubidium compared to potassium almost independently from the filter frequency, the mole-fraction behavior of heteromeric channels likely reflect simply the pore conductance with a nonlinearity due to different affinities for potassium and rubidium of the most external site in the conduction pathway. The dashed line in Fig. 12 was obtained by assuming a pore conductance that is a saturable function of the external cation and assuming a threefold larger affinity for potassium compared to rubidium (see the legend to Fig. 12).

Gating of homomeric KCNQ1 and heteromeric KCNQ1/KCNE1 channels are drastically different, and, to date, no satisfactory model that explains this difference has been proposed. Our previous study has shown that gating of homomeric KCNQ1, and especially the peculiar hook of tail currents, implies a gating model with at least two open states and a voltage-independent inactivation process (Pusch et al., 1998). Heteromeric KCNQ1/KCNE1 channels do not show a hook on repolarization under normal conditions. In many potassium channels, rubidium slows deactivation kinetics (e.g., Swenson and Armstrong, 1981; Cahalan et al., 1985; Matteson and Swenson, 1986; Sala and Matteson 1991; Shapiro and DeCoursey, 1991a,b). The effect of rubidium on the deactivation kinetics of heteromers is not a simple slowing: tail currents of heteromers become strongly sigmoidal in rubidium, whereas the slow time constant of the final deactivation time course is not significantly changed. The sigmoidicity develops with a considerable delay after depolarizing pulses. Such a behavior is qualitatively similar to the hook seen in homomeric channels, although heteromers have slower kinetics. Thus, the gating of heteromeric KCNQ1/KCNE1 channels is also likely represented by a gating scheme that includes at least two open states and an inactivated state with voltage-independent inactivation rates. However, to account for the slow kinetics of heteromers, several rate constants of such a scheme would have to be smaller. It could be that association with KCNE1 leads to an overall stiffer structure of the protein complex such that any conformational change that involves relatively large protein rearrangements is slowed. For a further understanding of the gating, it will be interesting to find out how mutations that are known to change specific gating properties in other potassium channels affect gating of homomeric KCNQ1 and heteromeric KCNQ1/KCNE1 channels.

Many types of voltage-dependent cation channels are complexes of a main pore-forming α subunit and one or more, generally smaller, auxiliary subunits. Often, association with these auxiliary subunits leads to modifications of gating properties, while leaving the conduction process itself unaffected. In contrast, the drastic effects of the association of KCNE1 with KCNQ1 on gating and permeation properties of the resulting potassium current has led several investigators to conclude that KCNE1 directly participates in pore-forming structures and modifies their conductive properties (Goldstein and Miller, 1991; Wang et al., 1996b; Tai and Goldstein, 1998; for review see Kaczmarek and Blumenthal, 1997). Our results further strengthen this hypothesis, suggesting, in particular, that KCNE1 interacts with the extracellular vestibule of the channel.

We thank Enrico Gaggero for construction of the voltage-clamp amplifier. The support by Telethon-Italy (grant 1079) is gratefully acknowledged.

REFERENCES

Ackerman, M. J. 1998. The long QT syndrome. *Pediatr. Rev.* 19:232–238.

Barhanin, J., F. Lesage, E. Guillemare, M. Fink, M. Lazdunski, and G. Romey. 1996. K(V)LQT1 and lsK (minK) proteins associate to form the I(Ks) cardiac potassium current. *Nature.* 384:78–80.

Cahalan, M. D., K. G. Chandy, T. E. DeCoursey, and S. Gupta. 1985. A voltage-gated potassium channel in human T lymphocytes. *J. Physiol.* 358:197–237.

Gambale, F., M. Bregante, F. Stragapede, and A. M. Cantù. 1996. Ionic channels of the sugar beet tonoplast are regulated by a multi-ion single-file permeation mechanism. *J. Membr. Biol.* 154:69–79.

Goldstein, S. A. N., and C. Miller. 1991. Site-specific mutations in a minimal voltage-dependent K^+ channel alter ion selectivity and open-channel block. *Neuron.* 7:403–408.

Heginbotham, L., and R. MacKinnon. 1993. Conduction properties of the cloned *Shaker* K^+ channel. *Biophys. J.* 65:2089–2096.

Kaczmarek, L. K., and E. M. Blumenthal. 1997. Properties and regulation of the minK potassium channel protein. *Physiol. Rev.* 77:627–641.

Matteson, D. R., and R. P. Swenson, Jr. 1986. External monovalent cations that impede the closing of K channels. *J. Gen. Physiol.* 87:795–816.

Pusch, M. 1998. Increase of the single-channel conductance of KvLQT1 potassium channels induced by the association with minK. *Pflügers Archiv.* 437:172–174.

Pusch, M., R. Magrassi, B. Wollnik, and F. Conti. 1998. Activation and inactivation of homomeric KvLQT1 potassium channels. *Biophys. J.* 75:785–792.

Sala, S., and D. R. Matteson. 1991. Voltage-dependent slowing of K channel closing kinetics by Rb^+. *J. Gen. Physiol.* 98:535–554.

Sanguinetti, M. C., M. E. Curran, A. Zou, J. Shen, P. S. Spector, D. L. Atkinson, and M. T. Keating. 1996. Coassembly of K(V)LQT1 and minK (IsK) proteins to form cardiac I(Ks) potassium channel. *Nature.* 384:80–83.

Schulze-Bahr, E., Q. Wang, H. Wedekind, W. Haverkamp, Q. Chen, Y. Sun, C. Rubie, M. Hördt, J. A. Towbin, M. Borggrefe, G. Assmann, X. Qu, J. C. Somberg, G. Breithardt,. C. Oberti, and H. Funke. 1997. KCNE1 mutations cause Jervell and Lange-Nielsen syndrome. *Nat. Genet.* 17:267–268.

Shapiro, M. S., and T. E. DeCoursey. 1991a. Selectivity and gating of the type L potassium channel in mouse lymphocytes. *J. Gen. Physiol.* 97: 1227–1250.

Shapiro, M. S., and T. E. DeCoursey. 1991b. Permeant ion effects on the gating kinetics of the type L potassium channel in mouse lymphocytes. *J. Gen. Physiol.* 97:1251–1278.

Sesti, F., and S. A. N. Goldstein. 1998. Single-channel characteristics of wild-type IKs channels and channels formed with two minK mutants that cause long QT syndrome. *J. Gen. Physiol.* 112:651–663.

Splawski, I., M. Tristani-Firouzi, M. H. Lehmann, M. C. Sanguinetti, and M. T. Keating. 1997. Mutations in the hminK gene cause long QT syndrome and suppress IKs function. *Nat. Genet.* 17:338–340.

Swenson, R. P., Jr, and C. M. Armstrong. 1981. K^+ channels close more slowly in the presence of external K^+ and Rb^+. *Nature.* 291:427–429.

Tai, K.-K., and S. A. N. Goldstein. 1998. The conduction pore of a cardiac potassium channel. *Nature.* 391:605–608.

Takumi, T., H. Ohkubo, and S. Nakanishi. 1988. Cloning of a membrane protein that induces a slow voltage-gated potassium current. *Science.* 242:1042–1045.

Tristani-Firouzi, M., and M. C. Sanguinetti. 1998. Voltage-dependent inactivation of the human K+ channel KvLQT1 is eliminated by association with minimal K^+ channel (minK) subunits. *J Physiol.* 510: 37–45.

Wagoner, K. P., and G. S. Oxford. 1987. Cation permeation through the voltage-dependent potassium channel in the squid axon. Characteristics and Mechanisms. *J. Gen. Physiol.* 90:261–290.

Wang, Q., M. E. Curran, I. Splawski, T. C. Burn, J. M. Millholland, T. J. VanRaay, J. Shen, K. W. Timothy, G. M. Vincent, T. de Jager, P. J. Schwartz, J. A. Toubin, A. J. Moss, D. L. Atkinson, G. M. Landes, T. D. Connors, and M. T. Keating. 1996a. Positional cloning of a novel potassium channel gene: KvLQT1 mutations cause cardiac arrhythmias. *Nat. Genet.* 12:17–23.

Wang, K.-W., K.-K. Tai, and S. A. N. Goldstein. 1996b. MinK residues line a potassium channel pore. *Neuron.* 16:571–577

Yang, W. P., P. C. Levesque, W. A. Little, M. L. Conder, F. Y. Shalaby, and M. A. Blanar. 1997. KvLQT1, a voltage-gated potassium channel responsible for human cardiac arrhythmias. *Proc. Natl. Acad. Sci. USA.* 94:4017–4021.

Yang, Y., and F. J. Sigworth. 1998. Single-channel properties of IKs potassium channels. *J. Gen. Physiol.* 112:665–678.